Magnetoresistance and Kohler rule in the topological chiral semimetal CoSi

A. E. Petrova, O. A. Sobolevskiy, and S. M. Stishov*
P. N. Lebedev Physical Institute, Leninsky prospekt 53, 119991 Moscow, Russia

(Received 7 September 2022; accepted 13 February 2023; published 21 February 2023)

The transverse and longitudinal magnetoresistance (MR) of two samples of the topological chiral semimetal CoSi with different residual resistivity ratios (RRRs) was studied. It is shown that the Kohler rule works for the transverse MR. The Kohler rule is also fulfilled in the case of longitudinal MR at a low reduced magnetic field. A sharp deviation in the longitudinal MR curve for the sample with low RRR from the Kohler prediction at high fields reveals its tendency to change sign at higher magnetic fields. We probably do not see any specific MR features connected to the topological chiral anomaly in the electron spectra of CoSi. This observation implies the need for certain revisions of the theoretical predictions. Shubnikov–de Haas quantum oscillations were observed and analyzed in both perpendicular and parallel configurations of the current and magnetic field in sample CoSi-1 with RRR = 9.33 at low temperatures.

DOI: 10.1103/PhysRevB.107.085136

I. INTRODUCTION

It is well known that for the majority of normal metals the transverse magnetoresistance (TMR) is proportional to H^2 in small fields, whereas the longitudinal magnetoresistance (LMR) is zero in the case of a spherical Fermi surface. However, in a general case, the LMR can also be significant and positive (see Refs. [1,2]). However, it has been recently proposed that in nonmagnetic Weyl semimetals the chiral anomaly leads to a novel kind of low-field LMR: negative and quadratic in the magnetic field [3,4]. Then the negative LMR phenomena were discovered in some topological chiral materials with Weyl points in the electron spectra (see Refs. [5–7]). So, the negative LMR may serve as a signature of the so-called chiral anomaly. A violation of the Kohler rule, which is a scaling law (magnetoresistance (MR) $= f[H/\rho_0]$) [1,2], can also be one of the features of topological chiral materials [8].

In this connection, the chiral semimetal CoSi is a subject of interest. CoSi belongs to the class of transition metal silicides and germanides with a noncentrosymmetric B20-type crystal structure. Interest in compounds of this kind has increased significantly due to their topological properties, which are determined by the specific symmetry of their crystal lattice. A violation of spatial symmetry in the B20 structure type causes the existence of special points, including Weyl points, in electronic and phonon spectra, characterized by topological Chern numbers (see Refs. [9,10]). At the same time, semimetals such as CoSi and RhSi, and, possibly, CoGe and RhGe, occupy a special position, revealing nontrivial fermions of various kinds [11,12]. CoSi is a diamagnetic semimetal with a very high residual resistance, which suggests the presence of a fairly large number of defects [13]. Currently, CoSi is being actively studied as a kind of model material demonstrating new types of Fermi quasiparticles (see Fig. 1, where the crystal and electron structures of CoSi are depicted). Note that the electronic properties of CoSi generally agree well with the calculations of the band structure and density of states, which are supported by angle-resolved photoemission spectroscopy (ARPES); see, for example, Ref. [14]).

Earlier, the MR in CoSi was studied in Refs. [15–17]. As was found in Refs. [15–17], the dependence of the MR on the magnetic field is described by the expression MR $\sim H^n$, where n varies from 1.6 to 1.8, which is different from the canonic $n = 2$ and probably reveals a trend to saturation. The Kohler rule is shown to work in the case of polycrystalline samples of CoSi when the zero-field resistivity is varied by temperature. No samples of CoSi with different residual resistivity were studied [15]. Slight negative-resistivity features were found in a strongly disordered sample of bulk CoSi [13], and claims of negative resistivity in single-crystalline CoSi nanowires [18] and CoSi thin films on silicon [19] should also be mentioned. With all that in mind, we decided to study the MR of the chiral semimetal CoSi, making use of two samples with different residual resistivity ratios (RRRs).

II. EXPERIMENT

Two samples of CoSi were selected for the current study. Sample CoSi-1, grown by the Czochralski method, with resistivity $\rho = 14.9$ μΩ cm at 2 K, has a size of approximately $0.4 \times 1.1 \times 9.5$ mm^3. Sample CoSi-2, grown by the Bridgman technique, with resistivity $\rho = 65.8$ μΩ cm at 2 K, has a size of approximately $0.7 \times 1.3 \times 7.5$ mm^3. Lattice parameters of the samples determined by powder x-ray diffraction are 4.444(1) Å (CoSi-1) and 4.443(1) Å (CoSi-2). Chemical analysis performed with an electron probe x-ray microanalyzer showed some deviation from the stoichiometric chemical composition (silicon deficiency 1%). Of the impurities that have been determined by atomic emission and mass spectroscopy, a noticeable amount of Ni (∼0.01%) was detected. Electrical transport measurements in magnetic fields up to 16 T were conducted using a Cryogen-Free Measurement System (CFMS-16) from Cryogenic. Magnetoresistance was measured with a four-probe ac method. A magnetic

*stishovsm@lebedev.ru

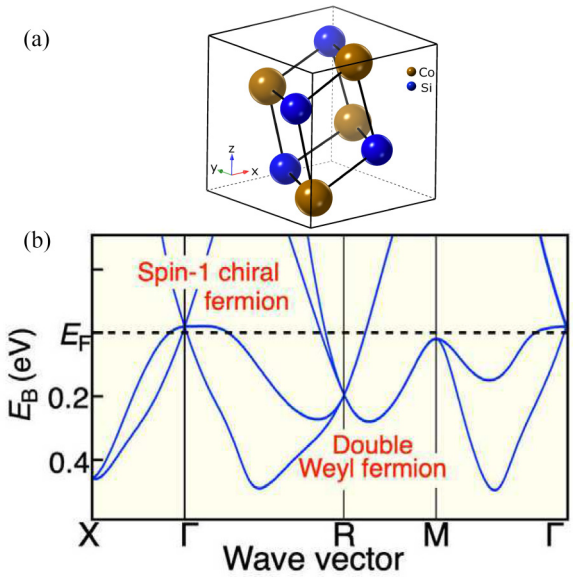

FIG. 1. (a) Crystal structure of CoSi. (b) Band structure of CoSi, redrawn from Ref. [14]. Spin-orbit splitting is not shown.

field was applied in two different orientations: parallel and perpendicular to the electrical current. Measurements were conducted in the following conditions: The electrical current was 500 μA, the measurement frequencies were 175.38 and 313.3 Hz for each sample, peak-to-peak noise was less than 40 nV, and the current and voltage wires were twisted in pairs, reducing noise in high magnetic fields. We used the Standard Research Current Source 580 and Lock-In SR 830. The temperature was measured with a Cernox temperature sensor. Temperature stability was about 10 mK.

The resistivities of samples are shown in Fig. 2. The high residual resistivity along with the low RRR and tendency to saturate at high temperatures place these samples in the

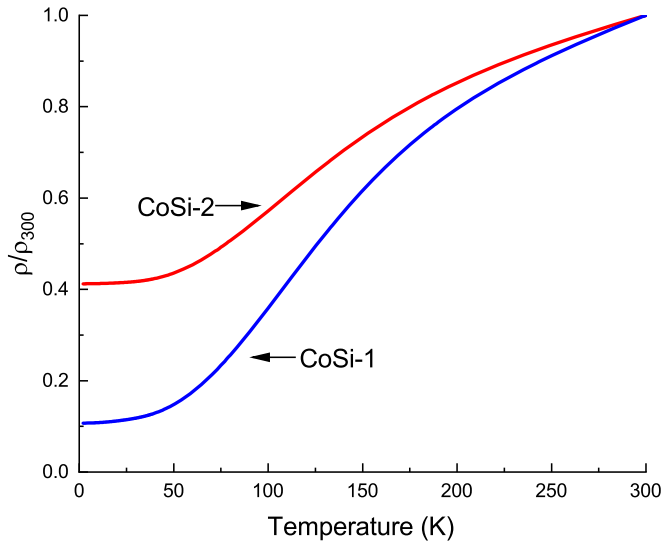

FIG. 2. Temperature dependence of the resistivity of the CoSi samples [captured on the y axis is the ratio of the temperature-dependent resistivity (ρ) and the resistivity at 300 K (ρ_{300})].

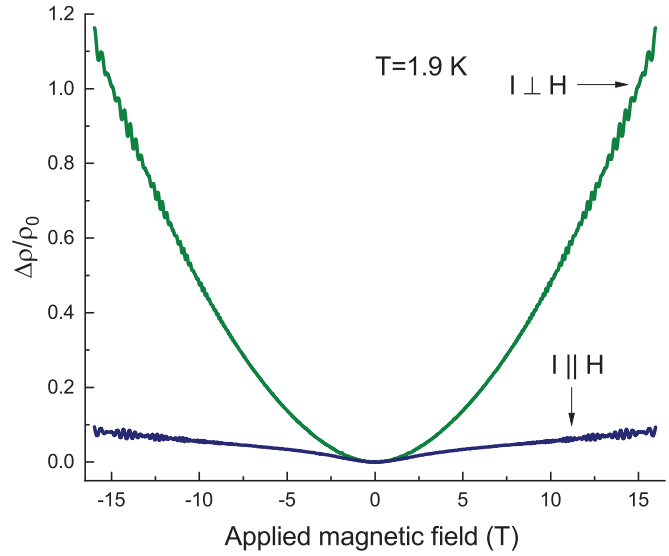

FIG. 3. Relative change in the resistivity of CoSi-1 in magnetic fields, corrected for the Hall contribution. Here and in the subsequent figures, captured on the y axis is $\Delta\rho/\rho_0 = \frac{\rho-\rho_0}{\rho_0}$, where ρ is the magnetic-field-dependent resistivity and ρ_0 is the resistivity at zero magnetic field.

category of so-called strongly disordered metals, whose resistivity can be described by a parallel resistor model [20].

The results of the magnetoresistance measurements, corrected for the Hall contributions arising due to the sample misalignments and not-quite-correct positions of the electrical contacts, are illustrated in Figs. 3 and 4.

III. RESULTS AND DISCUSSION

A simple data manipulation, taking into account that the MR is an even function of the magnetic field, permits a subtraction of the odd Hall contributions from the raw experimental data, which results in the corrected sets of the data

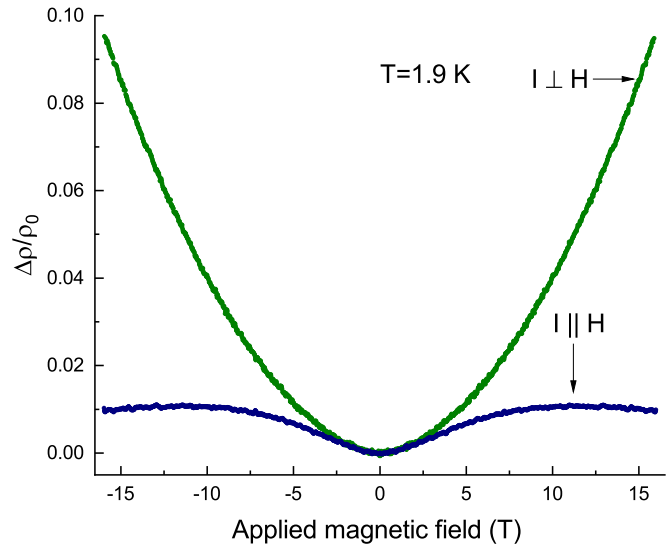

FIG. 4. Relative change in the resistivity of CoSi-2 in magnetic fields, corrected for the Hall contribution.

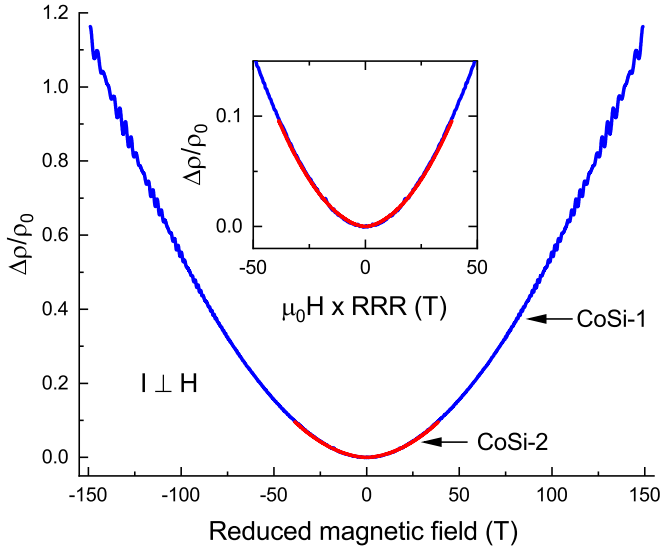

FIG. 5. Kohler plot for the TMR of samples CoSi-1 and CoSi-2. Here and in Fig. 6 the "reduced magnetic field" captured on the x axis is the value of the magnetic field $\mu_0 H$ multiplied by the RRR factor as a scaling coefficient [2].

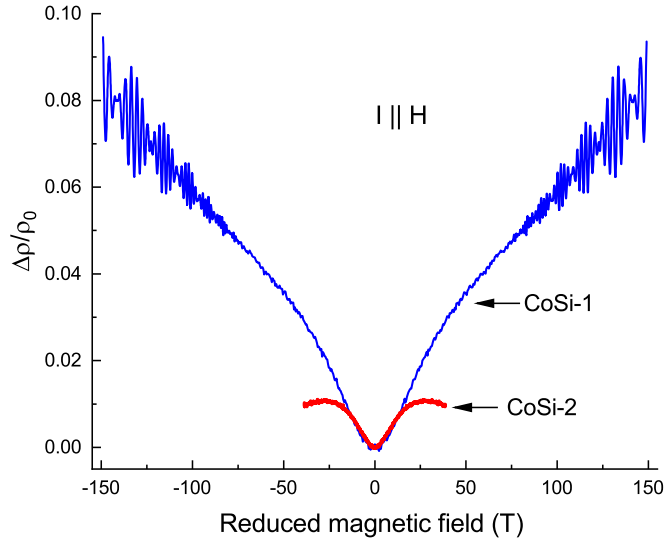

FIG. 6. Kohler plot for the LMR of samples CoSi-1 and CoSi-2.

illustrated in Figs. 3 and 4. These figures clearly demonstrate a lack of negative magnetoresistance in the LMR curves at least up to 15 T. However, as is seen in Figs. 3 and 4, the behavior of the LMR curves in magnetic fields is strongly different from that of the TMR ones. Moreover, the LMR for the high-resistivity sample, CoSi-2 (Fig. 4), supposedly may indicate a tendency for negative values of MR in much higher magnetic fields. Note that the mentioned tendency is revealed in sample CoSi-2, which does not support the quantum oscillations.

It should be pointed out that approximations of the TMR data (Figs. 3 and 4) by the expression MR $\sim H^n$ give an overall value of $n \cong 1.8$, in some agreement with data from Refs. [14–16]. The change in n from the theoretical value of 2 to the value of 1.8 may be the result of upcoming saturation.

Now we turn to an analysis of the Kohler rule, which is written in a standard form as $\frac{\rho-\rho_0}{\rho_0} = F(\frac{H}{\rho_0})$, where ρ_0-resistivity at $H = 0$, F-function, which does not depend on temperature, but change for different metals. A violation of the Kohler rule was observed for some topological materials in Ref. [8]. The authors of Ref. [8] suggested a modification of the Kohler rule in the form $\frac{\rho-\rho_0}{\rho_0} = F(\frac{H}{n_T \rho_0})$, where the coefficient n_T supposedly accounts for a change in the carrier density.

The Kohler plots for the two samples of CoSi, with quite different resistivities (see Fig. 2), are shown in Figs. 5 and 6. The Pippard approach was applied when RRR is used as a scaling coefficient [2]. As is evident, the Kohler rule works nicely for the TMR (Fig. 5). Surprisingly, the Kohler rule is also fulfilled in case of the LMR at low reduced magnetic field (Fig. 6). At the same time, a sharp deviation in the LMR curve for sample CoSi-2 from the Kohler prediction at high fields supports our conclusion about its tendency to change sign at higher magnetic fields (see Figs. 4 and 6). However, this feature is barely stipulated by the chiral anomaly. The point is that the LMR is a complicated and hardly universal function of the magnetic field [1]; that is why a fulfillment of the Kohler rule is normally observed in the case of the TMR. On the other hand, a peculiar negative MR can be seen in disordered metals due to the localization effects [13] as was suggested in Ref. [22]. At the same time we should mention the so-called "classical" mechanism for negative magnetoresistance [23,24]. Also, the "hydrodynamic" mechanism for negative magnetoresistance predicted years ago in Ref. [25] was discovered experimentally (see, for instance, Ref. [26]). So we probably do not see any specific MR features connected to the topological chiral anomaly in the electron spectra of CoSi. This observation implies the need for certain revisions of the theoretical predictions [3,4].

Finally, we cannot leave without attention to the resistance oscillations in magnetic fields clearly seen in the Figs. 3, 5, and 6. These oscillations are a revelation of the Shubnikov–de Haas quantum effect and can be observed in both the perpendicular and parallel configurations of the current and magnetic field of sample CoSi-1 with RRR = 9.33 at low temperatures. Sample CoSi-2 with RRR = 2.42 does not support the quantum oscillations because the electron mean free path is too short. Figure 7(a) demonstrates the oscillating part of the TMR resulting from subtracting the background from the MR curve (Fig. 3). The background was approximated with the "locally weighted polynomial regression" approach [27]. Two fundamental frequency peaks in the spectra arose after the fast Fourier transform [FFT; Fig. 7(b)]. The peak positions were determined from the Lorentzian fits. A similar procedure was performed for the LMR (Fig. 3), and two slightly different frequencies were obtained (see Table I).

The found frequencies correspond to the extremal cross-sectional area of almost-spherical electron pockets of the Fermi surface situated at the R point in the Brillouin zone (BZ) corner. These spheres are split by the spin-orbit coupling, which results in the observed two close frequencies (see Refs. [16,21]). The obtained data are shown in Table I, where some earlier results are also placed (see Refs. [16,17,21]) for the purpose of comparison. As seen in Table I the FFT peak frequencies slightly depend on the magnetic field direction,

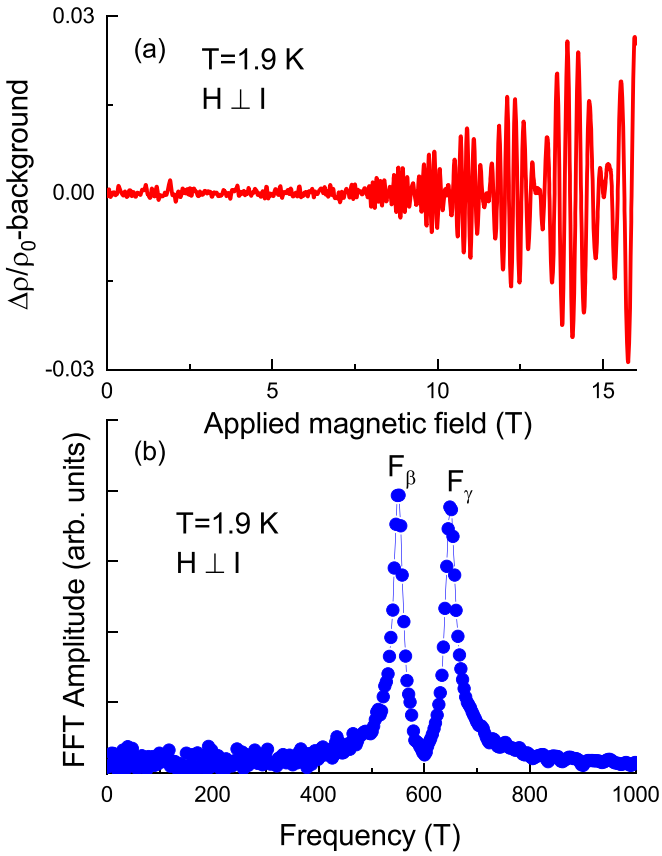

FIG. 7. Oscillating part of the TMR and corresponding FFT spectra for $H \perp I$. We borrowed the peak designations from Ref. [21], where the low-frequency peak $F\alpha$, corresponding to the Γ point, was also discovered.

which may imply some anisotropy of the Fermi surface. Indeed, as was shown in the de Haas–van Alphen study the electron pockets at the R point are not completely spherical [21]. Hence the orientational dependence of the oscillating frequencies may be real, despite the significant errors (1–3 T) connected with the frequency determinations. We also probably observed some temperature dependence of the oscillating frequencies in a way meaning that the spin-orbit splitting increases with temperature.

TABLE I. Frequencies (symbols ⊥ and ∥ indicate the magnetic field direction); values are in teslas.

$F\beta\gamma$	$1F\beta\perp$	$1F\gamma\perp$	$2F\beta\parallel$	$2F\gamma\parallel$
This paper	550.05	649.63	551.82	651.92
Ref. [16]	568	671		
Ref. [17]	563.9	664.6	564.5	664.1
Ref. [21]	557.6	656.7		

IV. CONCLUSIONS

The transverse (TMR) and longitudinal magnetoresistance (LMR) of two samples of the topological chiral semimetal CoSi with different RRRs was studied. It is shown that the Kohler rule works for the TMR. The Kohler rule is also fulfilled in the case of LMR at low reduced magnetic field. A sharp deviation in the LMR curve for the sample with low RRR from the Kohler prediction at high fields reveals its tendency to change sign at higher magnetic fields. However, we probably do not see any specific MR features connected to the topological chiral anomaly in the electron spectra of CoSi. This observation implies the need for certain revisions of the theoretical predictions [3,4].

Shubnikov–de Haas quantum oscillations were observed in both perpendicular and parallel configurations of the current and magnetic field in sample CoSi-1 with RRR = 9.33 at low temperatures. Two fundamental frequency peaks in the spectra arose after the fast Fourier transform was applied to the oscillation parts of the curves in Fig. 3, which is illustrated by Fig. 7. The same procedure was performed for the LMR (Fig. 5), and two slightly different frequencies were obtained (see Table I). These orientation-dependent frequency peaks probably indicate a slight anisotropy of the corresponding electron pockets in the BZ. The temperature dependence of the oscillating frequencies implies that the spin-orbit splitting probably increases with temperature.

ACKNOWLEDGMENTS

The authors gratefully acknowledge the technical support of V. A. Sidorov. The research was carried out at the LPI Shared Facility Center.

[1] F. J. Blatt, *Physics of Electronic Conduction in Solids* (McGraw-Hill, New York, 1968).
[2] A. B. Pippard, *Magnetoresistance in Metals* (Cambridge University Press, Cambridge, 1989).
[3] D. T. Son and B. Z. Spivak, Phys. Rev. B **88**, 104412 (2013).
[4] A. A. Burkov, Phys. Rev. B **91**, 245157 (2015).
[5] X. Huang, L. Zhao, Y. Long, P. Wang, D. Chen, Z. Yang, H. Liang, M. Xue, H. Weng, Z. Fang, X. Dai, and G. Chen, Phys. Rev. X **5**, 031023 (2015).
[6] C. Zhang, S.-Y. Xu, I. Belopolski, Zh. Yuan, Z. Lin, B. Tong, N. Alidoust, C.-C. Lee, S.-M. Huang, H. Lin, M. Neupane, D. S. Sanchez, H. Zheng, G. Bian, J. Wang, C. Zhang, T. Neupert, M. Z. Hasan, and S. Jia, Nat. Commun. **7**, 10735 (2016).
[7] Q. Li, D. E. Kharzeev, C. Zhang, Y. Huang, I. Pletikosic, A. V. Fedorov, R. D. Zhong, J. A. Schneeloch, G. D. Gu, and T. Valla, Nat. Phys. **12**, 550 (2016).
[8] J. Xu, F. Han, T.-T. Wang, L. R. Thoutam, S. E. Pate, M. Li, X. Zhang, Y.-L. Wang, R. Fotovat, U. Welp, X. Zhou, W.-K. Kwok, D. Y. Chung, M. G. Kanatzidis, and Z.-L. Xiao, Phys. Rev. X **11**, 041029 (2021).
[9] N. P. Armitage, E. J. Mele, and A. Vishwanath, Rev. Mod. Phys. **90**, 015001 (2018).
[10] D. Vanderbilt, *Berry Phases in Electronic Structure Theory: Electric Polarization, Orbital Magnetization, and Topological Insulators* (Cambridge University Press, Cambridge, 2019).

[11] P. Tang, Q. Zhou, and S. C. Zhang, Phys. Rev. Lett. **119**, 206402 (2017).
[12] G. Chang, S.-Y. Xu, B. J. Wieder, D. S. Sanchez, S.-M. Huang, I. Belopolski, T.-R. Chang, S. Zhang, A. Bansil, H. Lin, and M. Z. Hasan, Phys. Rev. Lett. **119**, 206401 (2017).
[13] S. M. Stishov, A. E. Petrova, V. A. Sidorov, V. N. Krasnorussky, and D. Mensel, Phys. Rev. B **86**, 064433 (2012).
[14] D. Takane, Z. Wang, S. Souma, K. Nakayama, T. Nakamura, H. Oinuma, Y. Nakata, H. Iwasawa, C. Cacho, T. Kim, K. Horiba, H. Kumigashira, T. Takahashi, Y. Ando, and T. Sato, Phys. Rev. Lett. **122**, 076402 (2019).
[15] S. Shanmukharao Samatham, D. Venkateshwarlu, and V. Ganesan, Mater. Res. Express **1**, 026503 (2014).
[16] X. Xu, X. Wang, T. A. Cochran, D. S. Sanchez, G. Chang, I. Belopolski, G. Wang, Y. Liu, H.-J. Tien, X. Gui, W. Xie, M. Z. Hasan, T.-R. Chang, and S. Jia, Phys. Rev. B **100**, 045104 (2019).
[17] D. S. Wu, Z. Y. Mi, Y. J. Li, W. Wu, P. L. Li, Y. T. Song, G. T. Liu, G. Li, and J. L. Luo, Chin. Phys. Lett. **36**, 077102 (2019).
[18] K. Seo, K. S. K. Varadwaj, P. Mohanty, S. Lee, Y. Jo, M.-H. Jung, J. Kim, and B. Kim, Nano Lett. **7**, 1240 (2007).
[19] S.-P. Chiu, S.-W. Chen, C.-T. Chen,R.-T. Wang, and J.-J. Lin (unpublished).
[20] H. Wiesmann, M. Gurvitch, H. Lutz, A. Ghosh, B. Schwarz, M. Strongin, P. B. Allen, and J. W. Halley, Phys. Rev. Lett. **38**, 782 (1977).
[21] H. Wang, S. Xu, X.-Q. Lu, X.-Y. Wang, X.-Y. Zeng, J.-F. Lin, K. Liu, Z.-Y. Lu, and T.-L. Xia, Phys. Rev. B **102**, 115129 (2020).
[22] P. A. Lee and T. V. Ramakrishnan, Rev. Mod. Phys. **57**, 287 (1985).
[23] A. Dmitriev, M. Dyakonov, and R. Jullien, Phys. Rev. B **64**, 233321 (2001).
[24] K. S. Denisov, K. A. Baryshnikov, P. S. Alekseev, and N. S. Averkiev, J. Phys.: Condens. Matter **33**, 385802 (2021).
[25] R. N. Gurzhi and S. I. Shevchenko, Sov. Phys. JETP **27**, 1019 (1968).
[26] J. Gooth, F. Menges, N. Kumar, V. Süß, C. Shekhar, Y. Sun, U. Drechsler, R. Zierold, C. Felser, and B. Gotsmann, Nat. Commun. **9**, 4093 (2018).
[27] G. Jēkabsons, Locally Weighted Polynomials toolbox for Matlab/Octave, 2016, available at http://www.cs.rtu.lv/jekabsons/.